CHINESE OPTICS LETTERS

Vol. 19, No. 11 | November 2021

Linearized wideband and multi-carrier link based on TL-ANN

Enji Liu (刘恩稷), Zhenming Yu (于振明)*, Zhiquan Wan (万智泉), Liang Shu (舒 亮), Kaixuan Sun (孙凯旋), Lili Gui (桂丽丽), and Kun Xu (徐 坤)

State Key Laboratory of Information Photonics and Optical Communications, Institute of Information Photonics and Optical Communications, Beijing University of Posts and Telecommunications, Beijing 100876, China

*Corresponding author: yuzhenming@bupt.edu.cn

Received December 29, 2020 | Accepted May 21, 2021 | Posted Online August 31, 2021

The analog photonics link (APL) is widely used in microwave photonics. However, in wideband and multi-carrier systems, the third inter-modulation distortion (IMD3) and cross-modulation distortion (XMD) will jointly limit the spurious-free dynamic range (SFDR) of links. In this paper, we experimentally present a linearized wideband and multi-carrier APL, in which the IMD3 and XMD are mitigated simultaneously by using artificial neural networks with transfer learning (TL-ANN). In this experiment, with different artificial neural networks, which are trained with the knowledge obtained from the two- or three-sub-carrier system, the IMD3 and XMD are suppressed by 21.71 dB and 11.11 dB or 22.38 dB and 16.73 dB, and the SFDR is improved by 13.4 dB or 14.3 dB, respectively. Meanwhile, compared with previous studies, this method could reduce the training time and training epochs to 16% and 25%.

Keywords: analog photonics link; modulation distortion; artificial neural networks; transfer learning.
DOI: 10.3788/COL202119.113901

1. Introduction

Microwave photonics (MWP) is regarded as an effective approach for realizing high quality transmission of 5G and beyond signals, and the conventional intensity modulation and direct detection (IMDD) analog photonic link (APL) gains considerable concern due to its brief construction and high commercial value. However, nonlinearity of electrical-optical conversion arouses severe distortion, which will degrade the spurious-free dynamic range (SFDR) of APL. Furthermore, in wideband and multi-carrier systems, in-band modulation distortion, like inter-modulation distortion (IMD), and out-band modulation distortion, like cross-modulation distortion (XMD), will jointly limit SFDR and degrade the linearization performance of links. Thus, investigating appropriate methods for improving SFDR is necessary[1,2].

Until now, many analog or digital approaches have been proposed to suppress these multi-source modulation nonlinear distortions[3–9]. However, analog methods usually suffer from complicated experiment setup or operations, and expensive devices result in high experiment cost. While digital methods need complex algorithm construction and have low compatibility, in recent years, the artificial neural network (ANN), which is regarded as a universal function approximator and does not rely on known models, has been widely used in optical communication, including optical performance monitoring, nonlinearity compensation, network fault prediction, and so on[10–14]. It becomes an effective method for compensating nonlinear distortions. ANN-based schemes show better performance compared with conventional analog or digital nonlinear compensation methods. However, in order to obtain great performance, the structure of the ANN usually has a complicated design, with too many hidden layers and neurons bringing high training cost, which largely decreases the practicability of ANNs. Therefore, how to decrease training cost is a worthy issue of study. Transfer learning (TL), which is a branch of machine learning, has been used in optical links in recent years[14]. According to the TL theory, knowledge could be transferred from one domain to another related domain[15]. Thus, we assume that low training cost and great compatible ability could be achieved by using the initialization that is based on pre-knowledge instead of random initialization when establishing an ANN. Compared with the combination of ANN and traditional pre-/post-digital methods, we consider that the combination of ANN and TL has low complexity and good compatibility.

In this Letter, we adopt ANN with TL (TL-ANN) as the digital signal processing (DSP) approach for APL linearization. We build up different APL-ANN systems, which contain two or three sub-carriers by simulation, and save the information of trained ANNs as pre-knowledge. Then, we experimentally demonstrate an APL-ANN system and transfer the pre-knowledge

from simulation ANNs to the ANN of the experiment. The results show that third IMD (IMD3) and XMD are suppressed by 21.71 dB and 11.11 dB with ANN based on the two sub-carrier system, while these distortions are suppressed by 22.38 dB and 16.73 dB with ANN based on the three sub-carrier system, and the SFDR is improved by 13.4 dB and 14.3 dB, respectively. The training time decreases from 3 h 19 min to 31 min, and the training epochs decrease from 2000 to 400. The training time reduces to 16%, and training epochs reduce to 25%.

2. Principle Description

Figure 1 shows a conventional IMDD APL. Two RF signals are injected into a Mach–Zehnder modulator (MZM). Then, the modulated optical signal with multi-source distortions is detected by a photo detector (PD). In frequency domain, the signal has various distortions with different frequencies. We assume ω_1, ω_2 and f_1, f_2 are the center frequencies of two dual-tone RF signals, respectively. The distortion terms like $\omega_1 \pm \omega_2$, $2\omega_{1,2} + \omega_{2,1}$ could be neglected, because these terms are far away from the fundamental frequency, but IMD3 terms are $2\omega_2 - \omega_1$ and $2\omega_1 - \omega_2$, and XMD terms are $f_1 + \omega_1 - f_2$, $f_1 + \omega_2 - f_2$, $f_2 + \omega_1 - f_1$, and $f_2 + \omega_2 - f_1$ when one out-band dual-tone RF signal works. These components are near the fundamental frequency and are hard to be mitigated by using filters. Therefore, in our system, we mainly mitigate IMD3 and XMD to realize the linearization of the link. In wideband and multi-carrier systems, XMD is the key factor of linearization performance, because the degree of deterioration will largely increase when the number of out-band signals is increasing.

In a conventional IMDD link, the delivery function can be presented as

$$x(t) = \frac{\Re P Z_{\mathrm{PD}}}{1 + \sin\theta}\left\{1 + \sin\left[\frac{\pi}{V_\pi} V_{\mathrm{RF}}(t) + \theta\right]\right\}. \tag{1}$$

$x(t)$ is the RF output, $\Re$, P, and Z_{PD} represent the responsivity, received optical power, and impedance of the PD, respectively, and θ and V_π represent the bias angle and switching voltage of the MZM.

For a wideband and multi-carrier link, we assume that the sub-carrier is centered at ω_k, and the amplitude and phase are A_k and θ_k. The multi-component RF signal is expressed as

$$V_{\mathrm{RF}}(t) = \sum_k A_k \cos(\omega_k t + \theta_k). \tag{2}$$

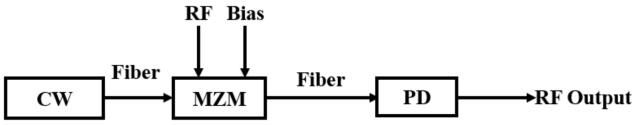

Fig. 1. IMDD link.

Combining Eqs. (1) and (2), the RF output of wideband and multi-carrier links can be achieved. In the frequency domain, the RF output exists with various distortions at different frequencies. The SFDR can be defined as the power range between the smallest fundamental frequency and the largest distortion component.

At the DSP stage, as shown in Fig. 2, we adopt an ANN with seven layers; it consists of an input layer, five hidden layers, and an output layer. Although multiple hidden layers will increase the complexity of network, the linearization performance is better. With the help of TL, the training cost could be substantially reduced, while the ANN will show good compatible ability. We adopt a purelin function as the transfer function for input and output neurons and the tansig function as an active function of hidden neurons. The inputs of ANN are RF modulated signals in the frequency domain, and the outputs represent recovered linearized signals in the frequency domain. The mitigation process could be divided into two phases; at the first stage, simulation modulated signals with higher power are used to train the neural network, and the performance analysis function and network learning function are the minimum mean square error method and gradient descent with momentum, respectively. After forward propagation, weights will back propagate to previous neurons in hidden layers until the error between the network output and expected output is under the set value. One epoch means that all of the training data experience a forward propagation and a back propagation. In order to quantify the training cost, we consider the training epoch and training time as vital termination parameters. In the second stage, we train new ANNs, which are initialized with information of pre-trained ANNs, and use experimental modulated signals to test the linearization performance of retrained networks.

The input, expected output, and network output of ANNs are f, $T(f)$, and $N(f)$, respectively. Therefore, the output $N_{i,k}(f)$ of the kth neuron in the ith hidden layer is given:

$$N_{i,k}(f) = \sum_{k=1}^{n} f[\omega_{t,k}^{i} x(f) + b_{i,k}]. \tag{3}$$

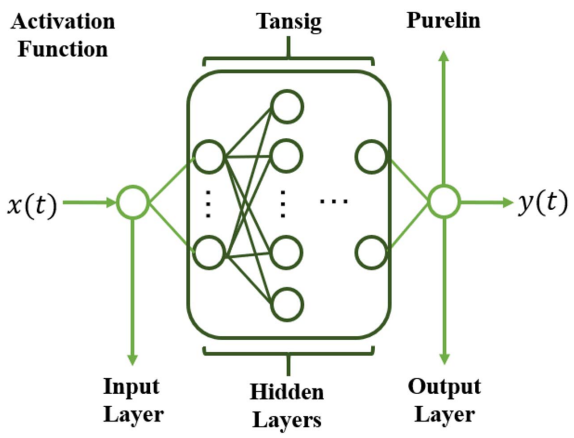

Fig. 2. ANN structure with multiple hidden layers.

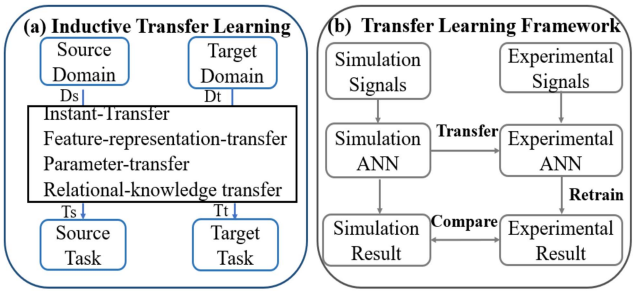

Fig. 3. TL scheme: (a) inductive TL and (b) TL aided ANN framework.

$\omega_{t,k}^{i}$ denotes the weight that connects the tth neuron in the $(i-1)$th hidden layer to the kth neuron in the ith hidden layer, and $b_{i,k}$ represents the bias of the kth neuron in the ith hidden layer. $f(\cdot)$ represents the transfer or activation function, and the error e is given as

$$e = \frac{1}{2}\left[N(f) - T(f)\right]^2. \tag{4}$$

Figure 3(a) shows the framework of TL. TL could be divided into three types: inductive TL, transductive TL, and unsupervised TL. In inductive TL, the source domain (Ds) and task domain (Dt) are known; meanwhile, the source task (Ts) and target task (Tt) are different but related, and the pre-knowledge, which is learned from the relation between the Ds and Ts, can be transferred to build the relation between the Dt and Tt by several methods, such as instant transfer and parameter transfer. In general, the simulated signal is more flexible and more accessible than the experimental signal; therefore, in the proposed TL-ANN, the signal of a simulated wideband and multi-carrier APL is in the Ds, and the Ts is the linearized signal. Through DSP with a multi-hidden layers ANN, a linearized APL can be achieved, and the distorted signal is linearized. Because of the similarities between the simulated signal and experimental signal, we assume the experimental signal is in the Dt, and the Tt is the linearization of the experimental signal. The knowledge, which was learned from the simulated ANN-APL system, can be used in the experimental ANN-APL system. Figure 3(b) shows the adopted transfer scheme. We firstly establish different simulated APLs and use the simulated signals to train different ANNs. Then, we initialize the ANN, which is adopted in the experimental system by using the knowledge of pre-trained ANNs, and the training time and training epoch of the ANN could largely decrease.

3. Results and Discussion

By the purpose of acquiring knowledge for TL, we build up different wideband and multi-carrier APLs by simulation. As shown in Fig. 4, we firstly adopt two dual-tone RF signals that have a difference of 15 GHz to emulate wideband and multi-carrier system and then add another dual-tone signal, which is centered at 10 GHz, to establish a more complicated system.

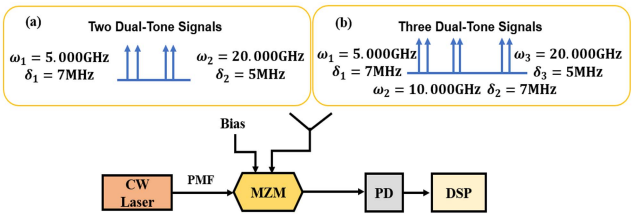

Fig. 4. Simulation setup of TL-ANN APL.

The target signal is centered at 5 GHz and spaced by $2\varphi_1 = 7$ MHz; the interference signals are selected at 10 GHz and spaced by $2\varphi_2 = 7$ MHz and 20 GHz and spaced by $2\varphi_3 = 5$ MHz, respectively. The power of the RF signals is settled as −8 dBm. As shown in Fig. 5, the suppression ratios in the two dual-tone signals case (2DSC) are 62.26 dB and 50.22 dB for IMD3 and XMD, respectively, while the least suppression ratio for IMD3 in the three dual-tone signals case (3DSC) is 18.79 dB, and the suppression ratio for XMD is 71.99 dB. As shown in Fig. 5(b), the distortions in 3DSC are more severe, new frequency components will appear, these components will superimpose as well, and the amplitudes of distortions will largely increase. After the FFT of the link output, we use the output of the simulation APL as the multi-layer network input, with the results of the trained ANN shown in Fig. 6. In 2DSC, the suppression ratios of the fundamental frequency to IMD3 and XMD are both above 85 dB, and the improvements are above 22.75 dB. While in 3DSC, the smallest suppression ratio gets an improvement above 38.86 dB, and other suppression ratios get improvements above 28.01 dB. We could notice that no matter whether it is in 2DSC or 3DSC, the multi-source distortions could be largely suppressed by ANN.

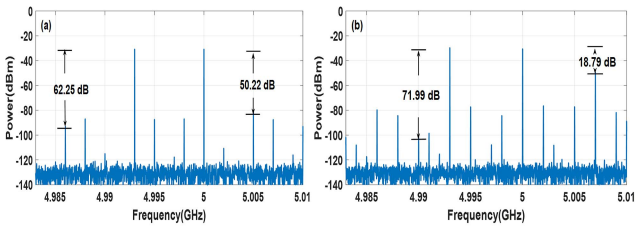

Fig. 5. RF power spectrum of modulation signals: (a) two dual-tone signals and (b) three dual-tone signals.

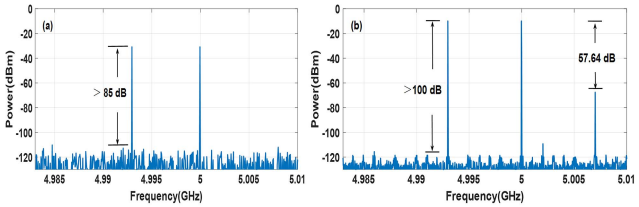

Fig. 6. RF power spectrum of processed signal: (a) two dual-signals and (b) three dual-tone signals.

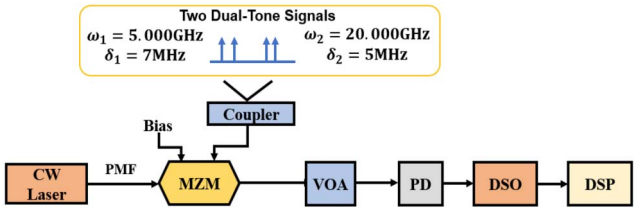

Fig. 7. Experimental platform setup.

The experimental platform is shown in Fig. 7, and, due to lack of a microwave generator, we adopt four microwave generators to generate two dual-tone signals, which have a difference of 15 GHz. The target RF signal is centered at 5 GHz and spaced by $2\varphi_1 = 7$ MHz, while the interference RF signal is centered at 20 GHz and spaced by $2\varphi_2 = 5$ MHz. A continuous wave laser generates an optical signal with the wavelength of 1550 nm and power of 16 dBm, and a short polarization-maintaining fiber is used to deliver the optical signal to an MZM, which is biased in the low bias region for maximum modulation efficiency. The RF signals are coupled by several large bandwidth RF combiners and injected into the MZM. Then, the modulated optical signal enters the PD through a variable optical attenuator (VOA). which decreases the optical power from 16 dBm to 0 dBm for preserving the stability of the link. After the PD, the detected signal is sampled by a digital signal oscilloscope (DSO) with 50 GS/s sampling rate, and the digital signal would be processed by an offline TL-ANN.

At the stage of DSP, we firstly adopt the sampled signal with RF input power of 15 dBm as the retraining input, then we initialize the ANN based on the knowledge of different pre-trained ANNs, and the results are shown in Fig. 8. In Fig. 8(a), various nonlinear distortions exist near the target frequency component, and the suppression ratios of the fundamental frequency to IMD3 and XMD are 35.26 dB and 40.74 dB, respectively. As shown in Figs. 8(b) and 8(c), the suppression ratios of the fundamental frequency to IMD3 and XMD are 56.97 dB and 51.85 dB with the retrained ANN, which is initialized with the knowledge of the pre-trained ANN that is based on 2DSC, and the suppression ratio improvements of IMD3 and XMD are 21.71 dB and 11.11 dB. With the retrained ANN, which is initialized with the knowledge of the pre-trained ANN that is based on 3DSC, the IMD3 and XMD suppression ratios are 57.64 dB and 57.47 dB, and the improvements are 22.38 dB and 16.73 dB. With different retrained ANNs, the multi-source distortions are both largely suppressed.

Then, we fix the target signal power at 15 dBm and scan the power of the interference RF signal from 15 dBm to 20 dBm. Several signals with various powers are adopted as the inputs of the two kinds of retrained ANNs (2DSC and 3DSC), and the results are shown in Fig. 9. With the increasing power of the interference RF signal, the XMD suppression ratios are decreased from 40.74 dB to 32.39 dB without retrained ANN, while the suppression ratios are decreased from 51.85 dB to 45.89 dB for the retrained ANN based on 2DSC and from 57.47 dB to 51.22 dB for the retrained ANN based on 3DSC,

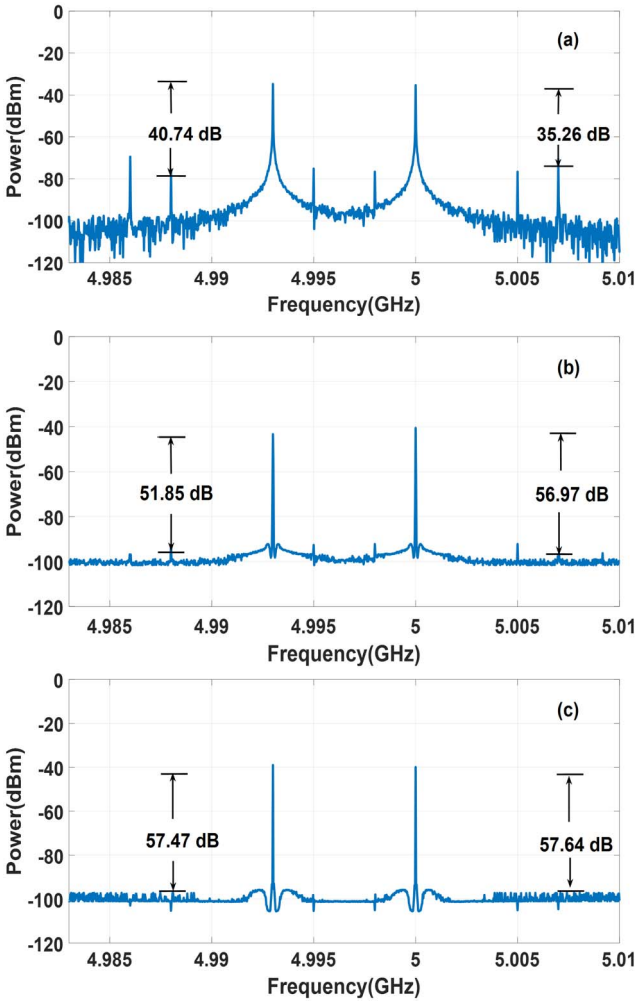

Fig. 8. RF power spectrum of target sidebands (a) before and (b) after ANN processing for 2DSC and (c) after ANN processing for 3DSC.

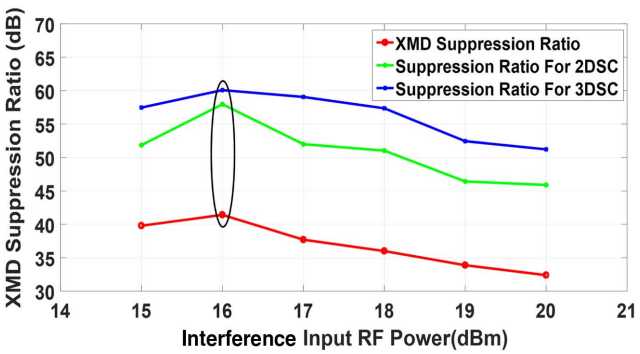

Fig. 9. Suppression ratios of XMD with change of interference input RF power.

respectively; the improvements of the suppression ratio are still above 10 dB. But, when the input power of the interference signal is 16 dBm, the collected data are distorted, so the suppression ratio is inaccurate.

The linearization performance of IMD3 is shown in Fig. 10, the measured noise floor with the analog-to-digital converter (ADC)

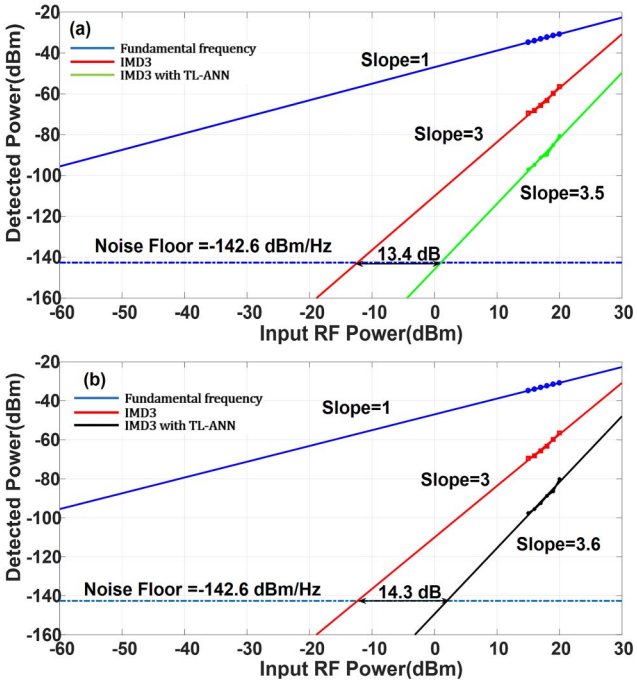

Fig. 10. Measured fundamental and IMD3 powers as a function of RF input power with ANN trained in (a) 2DSC and (b) 3DSC.

is −142.6 dBm/Hz, and the power of the target signal is changed from 15 dBm to 20 dBm. With the increase of RF power, the suppression ratios of the fundamental frequency component to IMD3 sidebands will decrease. After the linearization with the proposed TL-ANN, the improvement of SFDR is 13.4 dB with the retrained ANN based on 2DSC and 14.3 dB with the retrained ANN based on 3DSC, and the IMD3s are largely mitigated.

In previous work, the ANN shows good performance of linearization, but high training cost is a particle problem, and TL could be considered as one of the effective approaches that solves this problem. We use the parameters of pre-trained ANN to adjust the ANN that is used in the experiment system. In the retraining stage of ANN, the initial parameters of retrained ANNs are adjusted as the final parameters of pre-trained ANNs due to the similarities between pre-trained ANNs and retrained ANNs. The training cost of the retraining stage is much less than the pre-trained stage, the training time decreases from 3 h 19 min to 31 min, and the training epochs decrease from 2000 to 400. The training time is reduced to 16%, and the training epochs are reduced to 25%.

In this Letter, we use different retrained ANNs to test the compatibility of the proposed method. As shown in the results, the linearization performance with the retrained ANN based on 3DSC is better than the linearization performance with the retrained ANN based on 2DSC. Although the pre-training cost of ANN based on 3DSC is higher than that of ANN based on 2DSC, the re-training costs of different ANNs are almost same. This result means that we could train a complicated ANN for a complex situation in advance and apply the knowledge of ANN to solving simpler problems. The low training cost and good results could prove the compatibility of the proposed method.

4. Conclusion

In conclusion, a linearized wideband and multi-carrier APL, which is based on the ANN-TL, is experimentally presented. This scheme has good linearization performance and low training cost. In this Letter, we experimentally demonstrate that the IMD3 and XMD are suppressed by 21.71 dB and 11.11 dB with the retrained ANN based on 2DSC, while the IMD3 and XMD are suppressed by 22.38 dB and 16.73 dB with the retrained ANN based on 3DSC, and the SFDR is improved by 13.4 dB or 14.3 dB, respectively. Compared with previous APL-ANN systems, with the help of TL, the training time decreases from 3 h 19 min to 31 min, and the training epochs decrease from 2000 to 400. The training time reduces to 16%, and training epochs reduce to 25%. The proposed method shows good linearization performance and compatibility.

Acknowledgement

This work was supported in part by the National Key R&D Program of China (No. 2019YFB1803504), National Natural Science Foundation of China (Nos. 61901045, 61821001, and 61625104), Fundamental Research Funds for the Central Universities (No. 2019RC11), and State Key Laboratory of Information Photonics and Optical Communications (Beijing University of Posts and Telecommunications) (No. IPOC2019ZT04).

References

1. S. Lee, H. Kim, and J. Song, "Broadband photonic single sideband frequency up-converter based on the cross-polarization modulation effect in a semiconductor optical amplifier for radio-over-fiber system," Opt. Express **22**, 183 (2014).
2. X. Zhang, R. Zhu, D. Shen, and T. Liu, "Linearization technologies for broadband radio-over-fiber transmission system," Photonics **1**, 455 (2014).
3. A. Agarawal, T. Banwell, and T. K. Woodward, "Optically filtered microwave photonic links for RF signal processing applications," J. Lightwave Technol. **29**, 2394 (2011).
4. L. Daniel, M. F. Ali, B. Brandon, and J. Bahram, "Digital broadband linearization of optical links," Opt. Lett. **38**, 446 (2013).
5. Y. Cui, Y. Dai, F. Yin, J. Dai, K. Xu, J. Li, and J. Lin, "Intermodulation distortion suppression for intensity-modulated analog fiber-optic link incorporating optical carrier band processing," Opt. Express **21**, 23433 (2013).
6. A. Agarwal, T. Banwell, P. Toliver, and T. K. Woodward, "Predistortion compensation of nonlinearities in channelized RF photonics links using a dual-port optical modulator," IEEE Photon. Technol. Lett. **23**, 24 (2011).
7. X. Xie, Y. Dai, K. Xu, J. Niu, R. Wang, L. Yan, Y. Ji, and J. Lin, "Digital joint compensation of IMD3 and XMD in broadband channelized RF photonic link," Opt. Express **20**, 25636 (2012).
8. X. Liang, X. Liang, Y. Dai, K. Xu, F. Yin, J. Li, and J. Lin, "Mitigation of cross-modulation distortion in wideband analog photonic link based on digital post-processing," in *International Topical Meeting on Microwave Photonics and the 2014 9th Asia-Pacific Microwave Photonics Conference* (2014).
9. Y. Cai, Y. Ling, X. Gao, B. Xu, and K. Qiu, "Application of Kramers–Kronig receiver in SSB-OFDM-RoF link," Chin. Opt. Lett. **17**, 010605 (2019).

10. Z. Wan, J. Li, L. Shu, M. Luo, X. Li, S. Fu, and K. Xu, "Nonlinear equalization based on pruned artificial neural networks for 112-Gb/s SSB-PAM4 transmission over 80-km SSMF," Opt. Express **26**, 10631 (2018).
11. S. Liu, Y. Alfadhli, S. Shen, M. Xu, H. Tian, and G.-K. Chang, "A novel ANN equalizer to mitigate nonlinear interference in analog-RoF mobile fronthaul," IEEE Photon. Technol. Lett. **30**, 1675 (2018).
12. E. Liu, Z. Yu, C. Yin, and K. Xu, "Nonlinear distortions compensation based on artificial neural networks in wideband and multi-carrier systems," J. Quantum Electron. **55**, 8000305 (2019).
13. R. Wang, S. Xu, J. Chen, and W. Zou, "Ultra-wideband signal acquisition by use of channel-interleaved photonic analog-to-digital converter under the assistance of dilated fully convolutional network," Chin. Opt. Lett. **18**, 123901 (2020).
14. Y. Cheng, W. Zhang, S. Fu, and M. Tang, "Transfer learning simplified multi-task deep neural network for PDM-64QAM optical performance monitoring," Opt. Express **28**, 7607 (2020).
15. S. J. Pan and Q. Yang, "A survey on transfer learning," IEEE Trans. Knowl. Data Eng. **22**, 1345 (2010).